Pergamon

Int. J. Solids Structures Vol. 33, No. 9, pp. 1257–1269, 1996

0020–7683/96 $15.00 + .00

0020–7683(95)00094–1

STABILITY OF ELASTIC BARS ON UNCERTAIN FOUNDATIONS USING A CONVEX MODEL

C. P. PANTELIDES
Department of Civil Engineering, University of Utah, 3220 Merrill Engineering Building, Salt Lake City, UT 84112, U.S.A.

(*Received* 21 *October* 1994; *in revised form* 5 *April* 1995)

Abstract—A method is presented for evaluating the buckling load of weightless prismatic rigid bars resting on uncertain foundations which are modeled using linear extensional elastic springs. The uncertainty in the spring elements is expressed in terms of a nonprobabilistic convex model. An ellipsoidal bound is used which defines the uncertainty of the foundation in terms of a size parameter and the deviations of the elastic spring constants from their nominal values. The size parameter represents the size of the ellipsoid and is analogous to the standard deviation magnitude in probabilistic analyses. The semiaxes of the ellipsoid are the deviations of the foundation spring constants from their nominal values and they determine the shape of the ellipsoid. A first-order analysis shows that the reduction in the buckling load, when uncertainty in the foundation's spring stiffnesses is present, is a linear function of the size parameter and a nonlinear function of the semiaxes of the uncertainty ellipsoid. For the same uncertainty in the spring elements, different reductions in the buckling load result for beams with multimode buckling.

1. INTRODUCTION

Analysis of deterministic models is simpler than that of probabilistic models and in the former case results that are useful in design can readily be obtained. Deterministic models describe or predict the behavior of a structural system in which the outcome of an experiment or analysis under a specified set of conditions occurs with certainty. Probabilistic models are necessary when all that can be stated after studying many experiments or analyses is that a given outcome occurs in some fraction of the total number of the trials conducted. There is a tradeoff when detailed probabilistic information about a structural system is eliminated to gain computational ease. It is possible that the loss of accuracy in going from a probabilistic to a deterministic model is unacceptable. On the other hand, probabilistic models require extensive information about the random variables and distribution functions of the model.

The buckling of columns with random initial displacements, or columns randomly bent and initially twisted has been studied using Green's functions by Boyce (1961) and Bernard and Bogdanoff (1971), respectively. Elishakoff (1979) investigated the buckling of a stochastically imperfect column resting on a nonlinear elastic foundation using Monte Carlo simulation. Liaw and Yang (1989) studied the reliability of beam–columns with random geometric imperfections, uncertain material properties and uncertain moduli of elastic foundations. The buckling strength of end-restrained metal columns was investigated by Alibe (1990).

A new type of model for structural systems is one which represents uncertainty in a nonprobabilistic way. In this type of model, instead of using probabilistic procedures, an alternative method for analysis of uncertainty is used when a limited amount of information is available. This new type of model of structural systems with uncertainty is the convex model (Ben-Haim and Elishakoff, 1990). Convex models provide a completely nonprobabilistic representation of uncertainty and one does not have to think in a stochastic manner to construct them. A convex model of uncertainty is a set of functions specified by global characteristics such as input load functions, spectral properties, or functions of bounded energy. In effect, the convex model constrains uncertainty within a known bound.

In the problem of buckling of an elastic bar subject to axial compression with uncertain eccentricity, a convex model was constructed using the uncertainty in the eccentricities at the

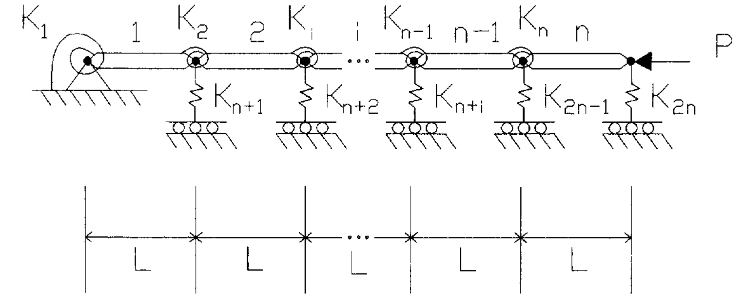

Fig. 1. n-bar system on Winkler foundation with uncertain rotational and extensional springs.

ends of the bar (Ben-Haim and Elishakoff, 1990). The relationship between the maximum bending moment in the bar vs a size parameter describing the convex model of uncertainty in the end eccentricities was obtained. In the buckling of thin-walled shells, which are sensitive to initial imperfections, a convex model was constructed from initial imperfection-sensitivity functions of cylindrical shells (Ben-Haim and Elishakoff, 1989). The aim of the analysis was to use fragmentary information about the initial imperfections of thin shells in order to determine the buckling loads which may be expected. Convex models have also been used to model uncertain imperfections in multimode dynamic buckling of cylindrical shells under symmetric radial impulsive loads (Lindberg, 1992a, 1992b). It was found that the maximum possible buckling deformations for any imperfection within uniform bounds could be made comparable to the buckling deformations from the probabilistic models at a reliability of 99.5%. The convex model has the advantage that its numerical evaluation and interpretation is much simpler than the probabilistic model. In addition, the convex model solution provides a means for quality control of each and every shell by simply recording the uniform bounds from imperfection measurements.

The dynamics of a thin shell under impact with limited deterministic information on its initial imperfections was investigated by Elishakoff and Ben-Haim (1990). The convex model was described in terms of the dominant initial imperfection Fourier coefficients within an ellipsoidal set. Convex models were also used to optimize the deployment of pressure sensors to detect uncertain slender obstacles on surfaces by Ben-Haim (1992). An energy-bound convex model was used to represent uncertainty in the initial deformation of a uniform beam (Ben-Haim, 1993a). The initial deformation energy determined both the degree of uncertainty in the initial beam shape and the maximum bending moment which the loaded beam can attain. A convex model has also been used to study the radial pulse buckling of shells in terms of initial geometrical imperfections in the shell shape (Ben-Haim, 1993b).

The concept of convex modeling provides an alternative way of analysis of uncertainty when a limited amount of information is available. Convex models specify uncertainties in the absence of detailed probabilistic information about the possible values of the variables of interest. The effect of modeling uncertainty by using convex vs probabilistic models has been studied by Ben-Haim (1994). The subjective design decisions which result when using convex models do not involve the element of chance in the sense that the concept of likelihood, which is inherent in probabilistic analyses, is not needed for convex models. In the present paper, convex models are used to evaluate the minimum buckling load for prismatic rigid bars resting on elastic springs of uncertain stiffness. The convex model is expressed in terms of uncertainty in the spring constants. A first-order analysis is performed assuming that the spectra of deviations of the spring constants vary within a convex ellipsoidal set.

2. STRUCTURAL MODEL

A system of n rigid bars each of length L is connected to the left support and to each other by n elastic frictionless rotational springs and is resting on n linear extensional elastic springs modeling the foundation as shown in Fig. 1. This model can be used to approximate

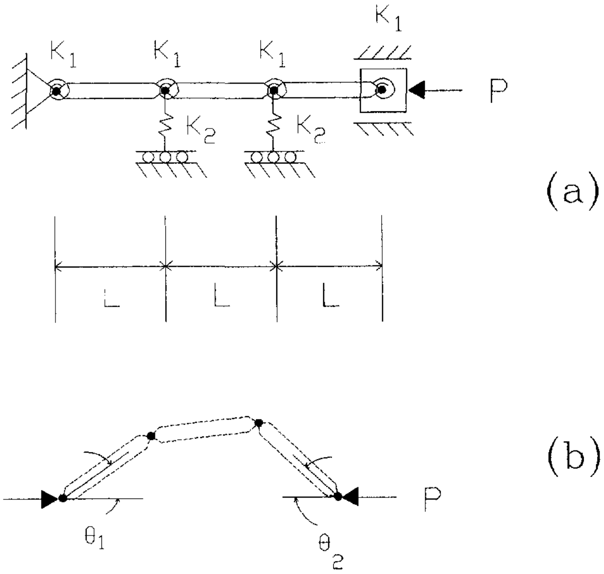

Fig. 2. Three-bar system with uncertain rotational and extensional springs: (a) system; (b) deflected position.

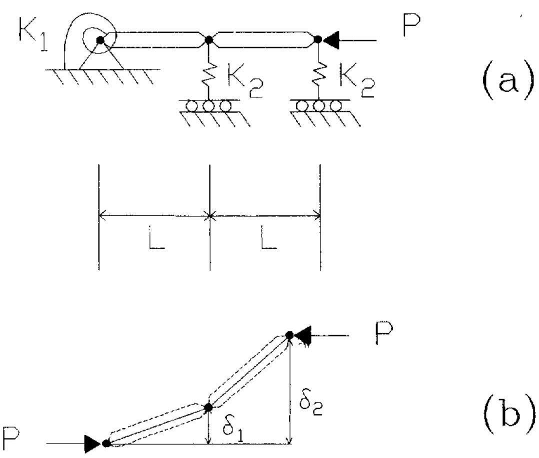

Fig. 3. Two-bar system with uncertain rotational and extensional springs: (a) system; (b) deflected position.

a weightless prismatic bar on a Winkler foundation. If the axial compressive load P is sufficiently large the system may buckle resulting in large rotations of the rotational springs. One can obtain the buckling loads P_i $(i = 1, \ldots, N)$ where N = number of degrees of freedom, using either bifurcation or energy approaches (Timoshenko and Gere, 1961; Langhaar, 1962; Chen and Lui, 1987). In buckling analysis, only the lowest critical load, P_1, is of interest. However, it should be noted that for the system of Fig. 2a the first mode critical load is the lowest for a certain range of values of spring stiffnesses k_1 and k_2, while the second mode critical load is the lowest for another range of k_1 and k_2.

The buckling load for the system shown in Fig. 1 can be found using the principle of stationary total potential energy. Let V be the total potential energy of a conservative system with enumerable degrees of freedom (N), such as the angles θ_i in Fig. 2b or the deflections δ_i in Fig. 3(b). The function V and its partial derivatives to the second-order are assumed as continuous functions. Using Taylor's theorem, the increment of V corresponding to increments h_i of angles θ_i is

$$\Delta V = \sum_{i=1}^{N} h_i V_i(\boldsymbol{\theta}) + \frac{1}{2!} \sum_{i=1}^{N} \sum_{j=1}^{N} h_i h_j V_{ij}(\boldsymbol{\theta}) + 0\,.(\boldsymbol{\theta})^3, \tag{1}$$

where the subscripts on V denote partial derivatives and $\boldsymbol{\theta}$ stands for all θ_i collectively; the third term denotes higher order terms that can be neglected. According to the principle of virtual work a necessary and sufficient condition for equilibrium is that the first term on the right hand side of eqn (1) vanishes. The second term on the right hand side of eqn (1) can also be expressed as

$$\sum_{i=1}^{N}\sum_{j=1}^{N} h_i h_j V_{ij}(\boldsymbol{\theta}) = \sum_{i=1}^{N}\sum_{j=1}^{N} a_{ij} h_i h_j, \tag{2}$$

where $a_{ij} = V_{ij}(\boldsymbol{\theta}')$ and $\boldsymbol{\theta}'$ = a point that is a solution of eqn (1). The coefficients a_{ij} are functions of the axial compressive load P. For a holonomic system, a necessary and sufficient condition to obtain the critical load is that the term in eqn (2) is positive semidefinite (Langhaar, 1962). This happens when the determinant of matrix $[a_{ij}]$ vanishes. The result is an expression for the buckling load in terms of the rotational and translational stiffnesses and the length L.

3. CONVEX MODEL

Consider the stiffness of the rotational and extensional springs k_i $(i = 1,\ldots, 2n)$ in Fig. 1 to be uncertain. The nominal values of the spring stiffnesses are k_i^0 $(i = 1,\ldots, 2n)$ and the deviations from these nominal values are ζ_i $(i = 1,\ldots, 2n)$. A convex model will be used to model the uncertainty in the spring stiffnesses. In this method, one determines the minimum buckling load when the uncertain values of the spring stiffnesses are confined within specified bounds. The convex model requires less information to define a certain bound than the information required to define a probability density function.

Ben-Haim and Elishakoff (1990), proposed a convex model in which the uncertain deviation from the perfect shape of a shell in terms of its initial imperfections was represented in terms of a convex set, **R**, of allowed functions. In order to minimize the buckling load, an infinite set of initial profiles was adopted on the basis of available data and the minimum of the buckling load on this set was sought. This infinite set of initial profiles is an extreme point set, **E**, whose convex hull is **R**. The pair of sets **E** and **R** is called a convex model. The ideas of extreme points and convex hulls are connected by a theorem which states that a closed and bounded and convex set in Euclidean space is the convex hull of its extreme points (e.g. Balakrishnan, 1981). The usefulness of this theorem is that the minimum of a linear function on a convex set can be found by searching the set **E** of extreme points instead of the entire domain. Instead of finding the buckling load at a certain reliability of probabilistically defined imperfections, one finds the buckling load for any imperfection shape constrained within a known bound.

A convex model is utilized for the buckling load of the structural model in Fig. 1. Assume that the deviations of the nominal values of the uncertain spring stiffnesses, i.e. ζ_i $(i = 1,\ldots, 2n)$, were measured and found to vary within the following ellipsoidal set:

$$\mathbf{Z}(\alpha, \omega_1\ldots, \omega_{2n}) = \left\{\zeta : \sum_{i=1}^{2n}\left(\frac{\zeta_i}{\omega_i}\right)^2 \leqslant \alpha^2\right\}, \tag{3}$$

where α = size parameter which determines the size of the ellipsoid and ω_i $(i = 1,\ldots, 2n)$ are the semiaxes which determine the shape of the ellipsoid. The values of α and ω_i $(i = 1,\ldots, 2n)$ can be obtained from measurements of the spring stiffnesses. Thus, as α increases the uncertainty in the values of the spring stiffnesses is increased. When $\alpha = 0$ the problem reduces to a deterministic one since no uncertainty in the spring stiffnesses exists. Equation (3) implies that the set $\mathbf{Z}(\alpha, \boldsymbol{\omega})$ is the convex hull of the ellipsoidal shell given as

$$\mathbf{A}(\alpha, \omega_1, \ldots, \omega_{2n}) = \left\{\zeta : \sum_{i=1}^{2n} \left(\frac{\zeta_i}{\omega_i}\right)^2 = \alpha^2\right\}. \tag{4}$$

The convex model developed in eqns (3) and (4) uses an ellipsoidal set of uncertainty. Other convex models are also possible such as an "envelope-bounded" function, in which the deviations of the nominal values of the uncertain spring stiffnesses may vary between lower and upper bounds.

4. FIRST-ORDER ANALYSIS USING THE CONVEX MODEL

The minimum buckling load of the system shown in Fig. 1 is required with respect to the uncertainty in the spring stiffnesses as expressed by the convex model of eqns (3) and (4). Define the function $P(\mathbf{k})$ to represent the buckling load for the system of Fig. 1. The length L of each bar is considered to be a deterministic constant and will not be included in the variables. The buckling load for uncertain spring stiffnesses to first order in ζ is:

$$P(\mathbf{k}^0+\zeta) = P(\mathbf{k}^0)+\sum_{i=1}^{2n} \frac{\partial P(\mathbf{k}^0)}{\partial k_i}\zeta_i, \tag{5}$$

where $\mathbf{k}^0$ are the normal values of the spring stiffnesses. It is desired to obtain the lower limit of the buckling load as ζ varies on the ellipsodial set defined by eqn (3). Define the first derivatives in eqn (5) as a vector $\mathbf{D}$ given by

$$\mathbf{D}^{\mathrm{T}} = \left[\frac{\partial P(\mathbf{k}^0)}{\partial k_1}, \frac{\partial P(\mathbf{k}^0)}{\partial k_2}, \ldots, \frac{\partial P(\mathbf{k}^0)}{\partial k_{2n}}\right], \tag{6}$$

where $(\ )^{\mathrm{T}}$ denotes the transpose of a vector. Following Ben-Haim and Eishakoff (1990), the lower limit of the buckling load is given by minimizing the buckling load in eqn (5), on the convex set $\mathbf{Z}$ given in eqn (3):

$$P_\mu(\alpha, \boldsymbol{\omega}) = \min_{\zeta \in \mathbf{Z}(\alpha,\omega)} [P(\mathbf{k}^0)+\mathbf{D}^{\mathrm{T}}\zeta] \tag{7}$$

where $\boldsymbol{\omega} = \{\omega_1, \ldots, \omega_{2n}\}$. Equation (7) implies that the minimum of the linear functional $\mathbf{D}^{\mathrm{T}}\zeta$ must be obtained on the convex set $\mathbf{Z}(\alpha, \boldsymbol{\omega})$. The minimum value of $P_\mu(\alpha, \boldsymbol{\omega})$ will occur on the set of extreme points of $\mathbf{Z}(\alpha, \omega)$, which is the collection of vectors $\mathbf{e} = \{e_1, \ldots, e_{2n}\}$ which satisfy eqn (4) identically.

Thus, the minimum buckling load becomes from eqn (7)

$$P_\mu(\alpha, \omega) = \min_{\mathbf{e} \in \mathbf{E}(\alpha,\omega)} [P(\mathbf{k}^0)+\mathbf{D}^{\mathrm{T}}\mathbf{e}] \tag{8}$$

Define $\boldsymbol{\Omega}$ as a $2n \times 2n$ diagonal matrix whose nonzero elements are equal to $1/\omega_i^2$, $(i = 1, \ldots, 2n)$. From eqn (4) the equality constraint can be restated as:

$$C(\mathbf{e}) \equiv \mathbf{e}^{\mathrm{T}}\boldsymbol{\Omega}\mathbf{e}-\alpha^2 = 0. \tag{9}$$

Using the method of Lagrange multipliers the Hamiltonian is defined for the minimization of $\mathbf{D}^{\mathrm{T}}\mathbf{e}$ in eqn (7) as (Papalambros and Wilde, 1988)

$$H(\mathbf{e}) = \mathbf{D}^{\mathrm{T}}\mathbf{e}+\lambda C(\mathbf{e}), \tag{10}$$

where λ = Lagrange multiplier constant and $\mathbf{D}$ was defined in eqn (6). For the minimum, the necessary conditions are:

$$\frac{\partial H}{\partial \mathbf{e}} = \mathbf{D}+2\lambda\mathbf{\Omega e} = \mathbf{0} \tag{11a}$$

$$\frac{\partial H}{\partial \lambda} = \mathbf{e}^{\mathrm{T}}\mathbf{\Omega e}-\alpha^2 = 0. \tag{11b}$$

It is obvious that eqn (11b) merely reproduces the constraint of eqn (9). Using eqns (11a) and (11b), the minimum value of **e** is found as

$$\mathbf{e}_{\min} = \pm\frac{\alpha\mathbf{\Omega}^{-1}\mathbf{D}}{\sqrt{\mathbf{D}^{\mathrm{T}}\mathbf{\Omega}^{-1}\mathbf{D}}}. \tag{12}$$

The minimum buckling load using a first order analysis and the negative sign in eqn (12) can be obtained from eqn (8) as

$$P_{\mu}(\alpha,\boldsymbol{\omega}) = P(\mathbf{k}^0)-\alpha\sqrt{\sum_{i=1}^{2n}\left(\omega_i\frac{\partial P(\mathbf{k}^0)}{\partial k_i}\right)^2}. \tag{13}$$

In eqn (13), **D** and **Ω** were substituted from eqns (6) and (9), respectively. It can be observed that the analysis has yielded an explicit expression between the minimum buckling load and the deviations from the nominal values of the spring stiffness constants as represented by the size parameter (α), and the semiaxes ($\omega_1\ldots,\omega_{2n}$). Equation (13) indicates that the buckling load is sensitive to both the size and shape of the ellipsoid. Significant reduction in the buckling load results from large sensitivity to springs whose semiaxes in the uncertainty ellipsoid are large. In addition, the minimum buckling load is reduced linearly with the overall size of the uncertainty in the spring constaints, α. To use the results derived in eqn (13) one must know or have some estimate of α which could be obtained from measurements. This is analogous to knowing the standard deviation magnitudes in probabilistic analyses.

5. ILLUSTRATIVE EXAMPLES

Two representative examples are given using the first-order approximation of eqn (13) for the buckling load of bars on elastic supports with uncertainty. These two examples are chosen so that analytical expressions of the buckling load with uncertain parameters can be obtained. For more complicated examples with a large number of degrees of freedom one must use computer techniques to obtain the results.

Example 1—spring-supported two-bar system

A two-bar system as shown in Fig. 3a, with one rotational spring of stiffness constant k_1 and two support springs of stiffness k_2 is analyzed. For this column, using δ_1 and δ_2 as generalized coordinates as shown in Fig. 3b, the strain energy in the springs is

$$U = \left(\frac{k_1}{L^2}+k_2\right)\frac{\delta_1^2}{2}+k_2\frac{\delta_2^2}{2}. \tag{14}$$

The potential energy of the external force, P, is

$$\Pi = \frac{P}{L}\left(\delta_1\delta_2-\delta_1^2-\frac{\delta_2^2}{2}\right) \tag{15}$$

and the total potential energy of the system is

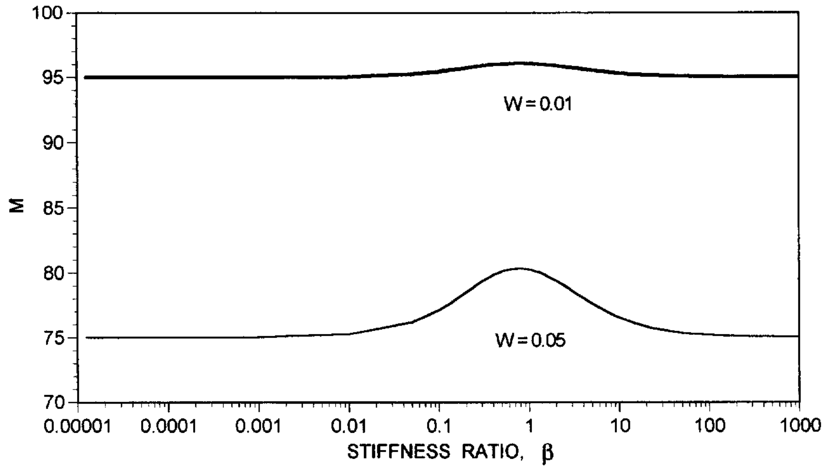

Fig. 4. Buckling load ratio for two uncertainty levels for example 1 ($\alpha = 5$).

$$V = U + \Pi. \tag{16}$$

Setting the determinant of matrix $[a_{ij}]$ defined in eqn (2) to zero gives the critical load as

$$\frac{P_{cr}L}{k_1} = \tfrac{1}{2}(1+3\beta-S) \tag{17a}$$

$$S = \sqrt{1+5\beta^2+2\beta}, \tag{17b}$$

where $\beta = k_2 L^2/k_1$ and P_{cr} = critical load. When the values of the spring stiffness constants k_1 and k_2 are uncertain, eqn (13) can produce the minimum buckling load directly. Evaluation of the partial derivatives $\partial P(\mathbf{k}^0)/\partial k_1$ and $\partial P(\mathbf{k}^0)/\partial k_2$ required in eqn (13) gives the minimum buckling load with consideration of uncertainty in k_1 and k_2 as

$$\frac{P_\mu(\alpha,\omega)L}{k_1} = \tfrac{1}{2}[1+3\beta-S] - \frac{\alpha}{2}\sqrt{W_1^2\left[1-\frac{(1+\beta)}{S}\right]^2 + W_2^2\left[3\beta-\frac{(\beta+5\beta^2)}{S}\right]^2}, \tag{18}$$

where $W_1 = \omega_1/k_1$, $W_2 = \omega_2/k_2$,β and S were defined earlier with respect to eqn (17). Note that W_1 and W_2 denote the normalized uncertainty semiaxes for the two spring constants with respect to their nominal values of k_1 and k_2, respectively.

To understand the implications of eqn (18), consider the ratio of the buckling load with uncertainty given by eqn (18) to that of the system without uncertainty given by eqn (17) in dimensionless form

$$M = \frac{P_\mu(\alpha,\omega)}{P_{cr}}. \tag{19}$$

A plot of this ratio is given in Fig. 4 as a function of the ratio of the two normalized stiffnesses, β. In Fig. 4 the values of the normalized semiaxes are assumed equal, i.e. $W_1 = W_2 = W$; the value of the size parameter is assumed as $\alpha = 5$. The nominal values of k_1 and k_2 were assumed as (Ting, 1982): $k_1^0 = 14{,}949$ kN-m rad^{-1} and $k_2^0 = 20{,}109$ kN m^{-1}. The length L was then varied to obtain the range of β displayed in Fig. 4 for $W_1 = W_2 = W$. It can be observed that the buckling load when uncertainty is present is reduced. For the case $W = 0.01$, the buckling load with uncertainty is between 95 and 96% of that of the system without uncertainty. For the case when $W = 0.05$, the buckling load with uncertainty is between 75 and 80.3% of that of the system without uncertainty. In both cases ($W = 0.01$ and $W = 0.05$) the value of β where the curves in Fig.

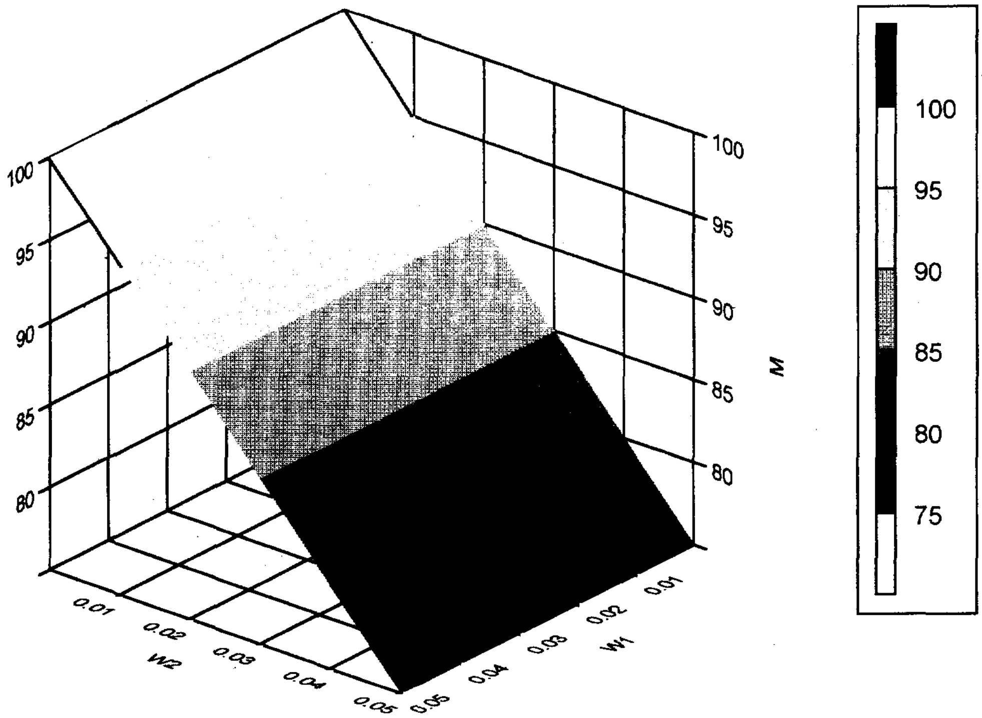

Fig. 5. Buckling load ratio for example 1 ($\alpha = 5$, $\beta = 200$).

4 attain a maximum is $\beta = 0.77$. The buckling load is a linear function of the size parameter, α, as implied by eqn (18). However, as Fig. 5 shows, the influence of the uncertainty in the translational springs (W_2) is far greater than that of the rotational spring (W_1). In Fig. 5, $\beta = 200$ and $\alpha = 5$ are used. In effect, Fig. 5 implies that the reduction in the buckling load when uncertainty is present for the structure of Fig. 3 is almost exclusively governed by the uncertainty W_2 of the translational springs k_2.

Example 2—spring-supported three-bar guided system

The bar system of Fig. 2a is considered with four rotational springs of stiffness k_1 and two translational support springs of stiffness k_2. Using θ_1 and θ_2 as the generalized coordinates, as shown in Fig. 2b, the strain energy in the springs is

$$U = k_1(3\theta_1^2+3\theta_2^2-4\theta_1\theta_2)+\frac{k_2L^2}{2}(\theta_1^2+\theta_2^2) \tag{20}$$

and the potential energy of the external force, P, is

$$\Pi = PL(\theta_1\theta_2-\theta_1^2-\theta_2^2). \tag{21}$$

The potential energy of the system, V, is the summation of U and Π. Evaluating the determinant of matrix $[\alpha_{ij}]$ for V defined in eqn (2) for this system, and setting it equal to zero gives

$$\frac{P_1L}{k_1} = 2+\beta \tag{22a}$$

$$\frac{P_2L}{k_1} = \tfrac{1}{3}(10+\beta), \tag{22b}$$

where $\beta = k_2L^2/k_1$. The two expressions in eqns (22a) and (22b) are plotted against the

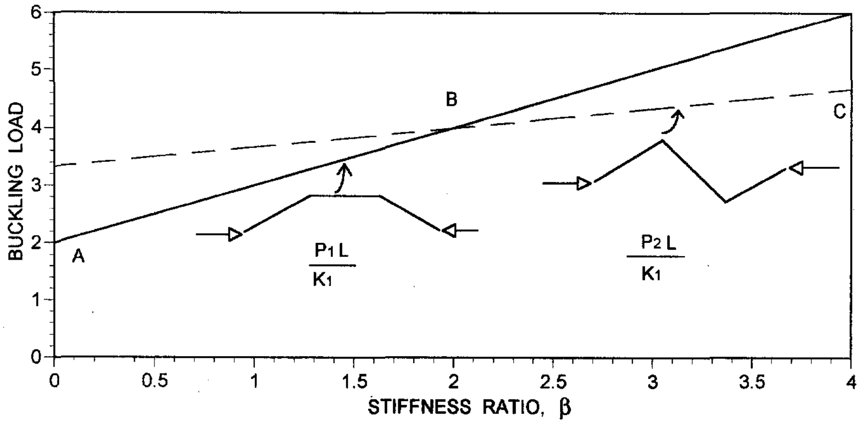

Fig. 6. Bimodal buckling load for three-bar system of example 2.

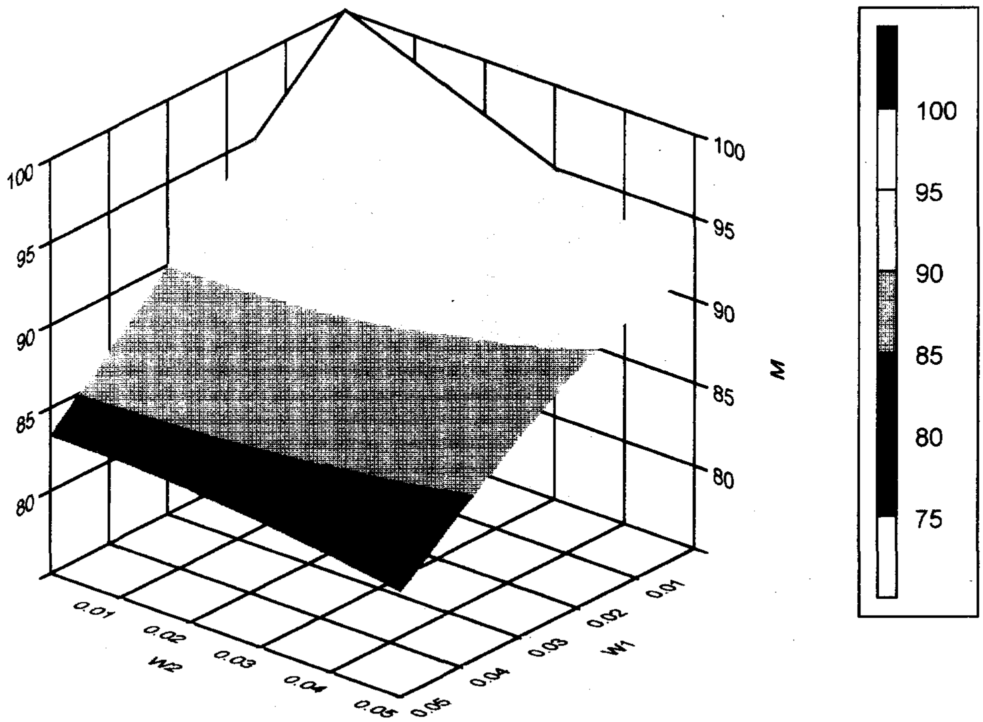

Fig. 7. Buckling load ratio for first mode of example 2 ($\alpha = 5$, $\beta = 1$).

stiffness ratio β in Fig. 6. It can be seen that for $\beta < 2$ (line AB) the first buckling mode (which is symmetric) governs with the buckling load as given in eqn (22a); for $\beta > 2$ (line BC) the second buckling mode (which is antisymmetric) governs with the buckling load as given in eqn (22b).

Case I. *First mode buckling.* In this case, applying eqn (13) the minimum buckling load with consideration of uncertainty in k_1 and k_2 is

$$\frac{P_{\mu 1}(\alpha, \omega)L}{k_1} = 2+\beta-\alpha\sqrt{4W_1^2+W_2^2\beta^2}, \tag{23}$$

where $W_1 = \omega_1/k_1$ and $W_2 = \omega_2/k_2$. A plot of the ratio of eqns (23) to (22a) is shown in Fig. 7 for $\beta = 1$, W_1 and W_2 from 0 to 5% and size parameter $\alpha = 5$. The uncertainty in k_1 as reflected by W_1 affects the buckling load considerably more than the uncertainty in k_2 as reflected by W_2. The reduction in the buckling load is a linear function of the size

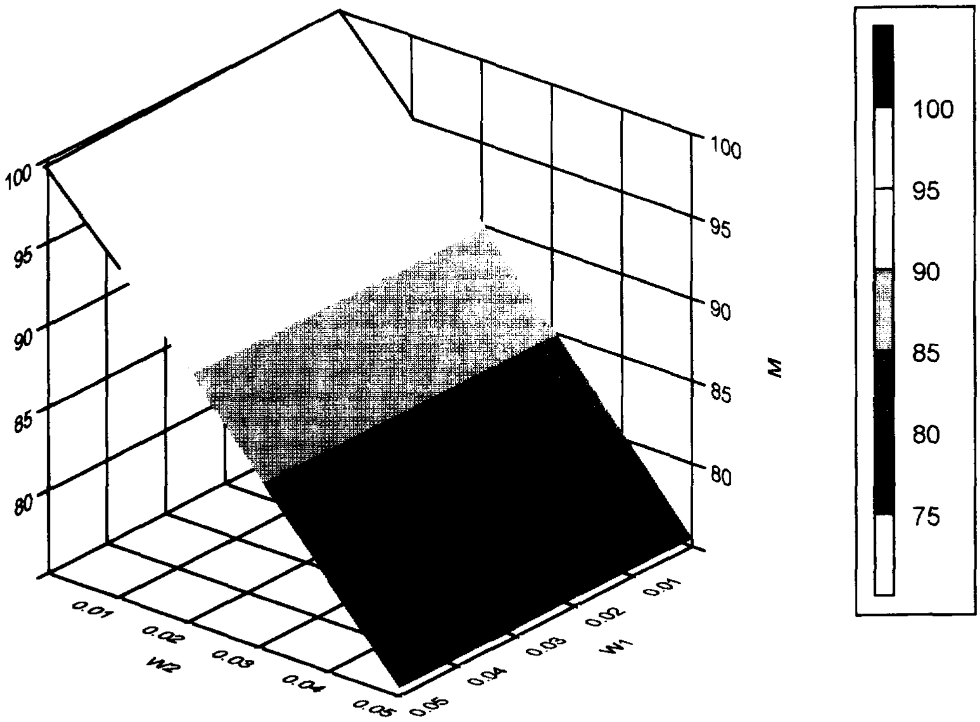

Fig. 8. Buckling load ratio for second mode of example 2 ($\alpha = 5$, $\beta = 450.204$).

parameter, α, as can be seen from eqn (23). Also, when $W_1 = W_2 = W$, the value of uncertainty semiaxis, W, is the slope of the straight line representing the buckling load reduction.

Case II. *Second mode buckling.* The minimum buckling load with consideration of uncertainty in k_1 and k_2 is obtained using eqn (13) as

$$\frac{P_{\mu 2}(\alpha, \omega)L}{k_1} = \tfrac{1}{3}(10+\beta-\alpha\sqrt{100W_1^2+W_2^2\beta^2}), \tag{24}$$

where as before $W_1 = \omega_1/k_1$ and $W_2 = \omega_2/k_2$ are the normalized uncertainty semiaxes for the two spring constants with respect to the nominal values of k_1 and k_2. A plot of the ratio of eqn (24) to (22b) for this case is shown in Fig. 8 for values of W_1 and W_2 from 0 to 5%, size parameter $\alpha = 5$, and $\beta = 450.204$. This value was chosen from actual data for beams on elastic foundation (Ting, 1982). From this graph and eqn (24) it is obvious that the uncertainty in k_2 affects the buckling load more than the uncertainty in k_1 for $\beta > 10$. It is interesting to note that whereas for the first mode buckling the uncertainty in the rotational springs is dominant, in the second mode buckling (for $\beta > 10$) the uncertainty in the translational support springs is dominant. The reduction in the buckling load is a linear function of the size parameter α and when the uncertainty semiaxes are equal ($W_1 = W_2 = W$), W represents the slope of the straight line reduction in the buckling load. In comparing Cases I and II, it can be seen that for the same levels of uncertainty in the spring constants, the reduction in the buckling load is more pronounced in the second-mode buckling.

The difference between first mode buckling (Case I) and second mode buckling (Case II) depends on β and is shown in Fig. 9. Figure 9 shows the ratio of the buckling load with uncertainty of eqns (23) and (24) as a percentage of the buckling load without uncertainty of (22a) and (22b), respectively, for $W_1 = W_2 = W = 0.01$, $W = 0.05$ and $\alpha = 5$. It is obvious that when uncertainty is present, the second mode buckling load is reduced differently from the first mode buckling load.

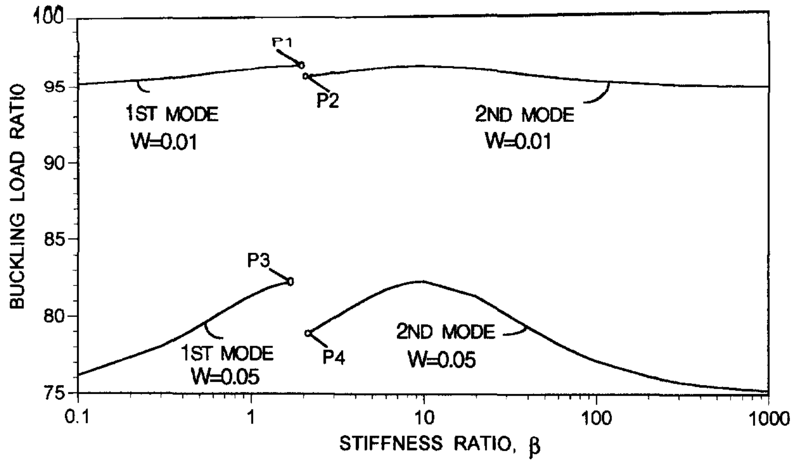

Fig. 9. Buckling load ratio for both modes of example 2 as a function of the stiffness ratio ($\alpha = 5$).

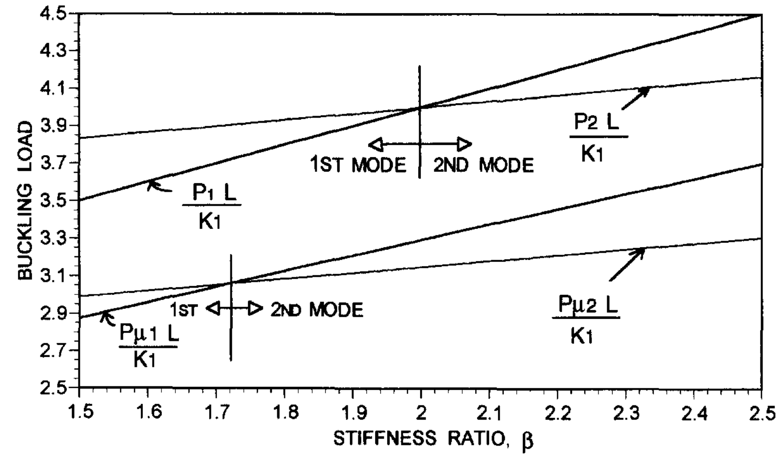

Fig. 10. Buckling load for three-bar system of example 2 with and without uncertainty ($W_1 = W_2 = 0.05$, $\alpha = 5$).

Figure 9 suggests a type of imperfection-sensitive bifurcation. The transition point, β_t, from first to second mode buckling when uncertainty is present, is found by equating the values of $P_{\mu 1}$ and $P_{\mu 2}$ in eqns (23) and (24), respectively. For $W_1 = W_2 = W = 0.01$ the transition point is at P_1 and its value is $\beta_t = 1.955$; when $W_1 = W_2 = W = 0.05$ the transition point is at P_3 and its value is $\beta_t = 1.721$. Points P_2 and P_4 in Fig. 9 are the transition points from first to second mode buckling for the system without uncertainty ($\beta_t = 2$).

Since Fig. 9 shows the buckling load ratio, rather than the buckling load, it is rather difficult to illustrate what occurs near $\beta = 2$. The behavior of the imperfection-sensitive bifurcation near $\beta = 2$ from eqns (22a) and (22b) for the buckling load without uncertainty and from eqns (23) and (24) for the buckling load with uncertainty is shown in Fig. 10. The uncertainty is defined in terms of the normalized uncertainty semiaxes $W_1 = W_2 = W = 0.05$ and the size parameter $\alpha = 5$. Figure 10 shows that the buckling load is reduced significantly when uncertainty is present. In addition, the transition point from first to second mode buckling occurs at a lower value of $\beta_t = 1.721$. If the values of the uncertainty semiaxes are assumed equal, i.e. $W_1 = W_2 = W$, from eqns (23) and (24) the values of the transition stiffness ratios are a function of the product αW. Figure 11 shows the values of the transition stiffness ratios from first to second mode buckling, when uncertainty is present, as a function of αW. It is obvious that the transition from first to second mode buckling occurs for lower values of β_t when uncertainty is present.

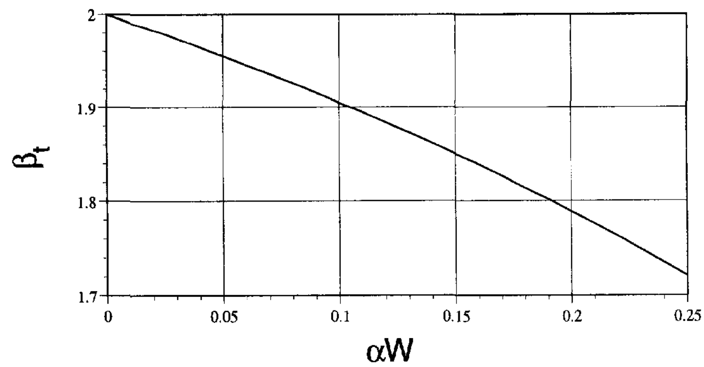

Fig. 11. Transition stiffness ratio from first-mode to second-mode buckling for three-bar system of example 2 in the presence of uncertainty.

6. CONCLUDING REMARKS

The buckling load of weightless prismatic bars in the presence of uncertainty in the rotational connecting springs and translational support spring elements is evaluated using a nonprobabilistic convex model. Explicit expressions are derived for the buckling load in terms of the deviations of the rotational and translational spring stiffness constants from their nominal values. The uncertainty in the stiffness constants of the rotational and translational springs is expressed as an ellipsoidal set defined in terms of the uncertainty of each spring as a semiaxis of the ellipsoid. The convex model is defined in terms of a size parameter which determines the size of the ellipsoidal set. As the size parameter increases, the uncertainty in the values of the spring constants is increased. If the size parameter equals zero the problem is reduced to a deterministic buckling problem. This makes the method attractive since it does not require probabilistic distribution descriptions of the uncertain parameters. Results from a first-order analysis show that the reduction in the buckling load, when uncertainty in the spring stiffnesses is present, is a linear function of the size parameter and a nonlinear function of the semiaxes of the uncertainty ellipsoid. The reduction in the buckling load varies significantly with the uncertainty of the spring constants.

For systems of bars for which the buckling mode depends on the values of the translational and rotational spring constants, different reductions in the buckling load result for the same level of uncertainty in the stiffness of the spring elements. For a certain buckling mode the uncertainty in the rotational springs is dominant, while for another mode the uncertainty in the translational springs is dominant in determining the buckling load reduction. The transition stiffness ratio at which buckling from one mode switches to the other was found in terms of the uncertainty semiaxes and the size parameter. The value of the transition stiffness ratio is reduced as the uncertainty is increased. It is interesting that this bifurcation from first to second mode buckling as a result of substrate uncertainty is so readily analyzed using the convex model approach.

Acknowledgements—Financial support by the National Science Foundation through grant MSS-9207252 is gratefully acknowledged. The author would like to thank the reviewers for their comments. The author would like to acknowledge the constructive suggestions made by Professor Yakov Ben-Haim of Technion. The author also acknowledges the assistance of Ms Beverly La Roe who typed the manuscript.

REFERENCES

Alibe, B. (1990). Characteristics of columns with uncertain end restraint. *J. Struct. Engng, ASCE* **116,** 1522–1534.
Balakrishnan, A. V. (1981). *Applied Functional Analysis*, 2nd Edn. Springer, New York.
Ben-Haim, Y. (1992). Convex models for optimizing diagnosis of uncertain slender obstacles on surfaces. *J. Sound Vibr.* **152,** 327–341.
Ben-Haim, Y. (1993a). Failure of an exially compressed beam with uncertain initial deflection of bounded strain energy. *Int. J. Engng Sci.* **31,** 989–1001.
Ben-Haim, Y. (1993b). Convex models of uncertainty in radial pulse buckling of shells. *ASME J. Appl. Mech.* **60,** 683–688.
Ben-Haim, Y. (1994). A non-probabilistic concept of reliability. *Struct. Safety* **14,** 227–245.

Ben-Haim, Y. and Elishakoff, I. (1989). Non-probabilistic models of uncertainty in the non-linear buckling of shells with general imperfections: theoretical estimates of the knock down factor. *ASME J. appl. Mech.* **111,** 403–410.

Ben-Haim, Y. and Elishakoff, I. (1990). *Convex Models of Uncertainty in Applied Mechanics*. Elsevier, New York.

Bernard, M. C. and Bogdanoff, J. L. (1971). Buckling of columns with random initial displacements. *J. Engng Mech. ASCE* **97,** 755–771.

Boyce, W. (1961). Buckling of a column with random initial displacements. *J. Aeronaut. Sci.* **28,** 308–312.

Chen, W. F. and Lui, E. M. (1987). *Structural Stability: Theory and Implementation*. Elsevier, New York.

Elishakoff, I. (1979). Buckling of a stochastically imperfect finite column on a nonlinear elastic foundation—a reliability analysis. *J. Aeronaut. Sci.* **28,** 308–312.

Elishakoff, I. and Ben-Haim, Y. (1990). Dynamics of a thin cylindrical shell under impact with limited deterministic information on its initial imperfections. *Int. J. Struct. Safety* **8,** 103–112.

Langhaar, H. L. (1962). *Energy Methods in Applied Mechanics*. Wiley, New York.

Liaw, D. G. and Yang, H. T. Y. (1989). Reliability of randomly imperfect beam-columns. *J. Engng Mech. ASCE* **115,** 2251–2270.

Lindberg, H. E. (1992a). An evaluation of convex modeling for multimode dynamic buckling. *ASME J. Appl. Mech.* **59,** 929–936.

Lindberg, H. E. (1992b). Convex models for uncertain imperfection control in multimode dynamic buckling. *ASME J. Appl. Mech.* **59,** 937–945.

Papalambros, P. Y. and Wilde, D. J. (1988). *Principles of Optimal Design*. Cambridge University Press, New York.

Timoshenko, S. P. and Gere, J. M. (1961). *Theory of Elastic Stability*. McGraw-Hill, New York.

Ting, B. Y. (1982). Finite beams on elastic foundation with restraints. *J. Struct. Engng. ASCE* **108,** 611–621.